The Transcriptional Regulation and Ubiquitination Dependent Regulation of Hnrnpk Oncogenic Function in Prostate Tumorigenesis

Huan-Lei Wu
Tongji Hospital of Tongji Medical College of Huazhong University of Science and Technology
Sen-Mao Li
Tongji Hospital of Tongji Medical College of Huazhong University of Science and Technology
Yao-chen Huang
Tongji Hospital of Tongji Medical College of Huazhong University of Science and Technology
Qi-Dong Xia
Tongji Hospital of Tongji Medical College of Huazhong University of Science and Technology
Peng Zhou
Tongji Hospital of Tongji Medical College of Huazhong University of Science and Technology
Xian-Miao Li
Tongji Hospital of Tongji Medical College of Huazhong University of Science and Technology
Xiao Yu
Tongji Hospital of Tongji Medical College of Huazhong University of Science and Technology
Shao-Gang Wang
Tongji Hospital of Tongji Medical College of Huazhong University of Science and Technology
Zhang-Qun Ye
Tongji Medical University: Tongji Medical College
Jia Hu (jiahutjm@163.com)
Tongji Hospital of Tongji Medical College of Huazhong University of Science and Technology

Research

Keywords: hnRNPK, Prostate cancer, miRNA, Post-transcriptional regulation, degradation

Posted Date: May 7th, 2021

DOI: https://doi.org/10.21203/rs.3.rs-452319/v1

Version of Record: A version of this preprint was published at Cancer Cell International on December 1st, 2021. See the published version at https://doi.org/10.1186/s12935-021-02331-x.

Abstract

Background

Heterogeneous nuclear ribonucleoprotein K (hnRNPK) is a nucleic acid-binding protein that regulates diverse biological events. Pathologically, hnRNPK proteins are frequently overexpressed and clinically correlated with poor prognosis to various types of human cancers, therefore pursued as attractive therapeutic targets for selective patients. However, both the transcriptional regulation and degradation of hnRNPK in prostate cancer are remain poorly understood.

Methods

qRT-PCR was used to detect the expression of hnRNPK and miRNA; Immunoblots and immunohistochemical assays were used to determine the levels of hnRNPK and other proteins. Flow cytometry was used to investigate cell cycle stage. MTS and clonogenic assays were used to investigate cell proliferation. Immunoprecipitation was used to analyze the interaction between SPOP and hnRNPK. A prostate carcinoma xenograft mouse model was used to detect the in vivo effects of hnRNPK and miRNA.

Results

In the present study, we observed that hnRNPK emerged as an important player in carcinogenesis process of PrCa. miR-206 and miR-613 suppressed hnRNPK expression by targeting the 3'-UTR of hnRNPK in PrCa cell lines, where hnRNP K is overexpressed. In biological effects studies, proliferation and colony formation of PrCa cells in vitro, and tumor growth in vivo, were also dramatically suppressed upon reintroduction of miR-206/ miR-613. We have further provided clear evidence that Cullin 3 SPOP as a novel upstream E3 ubiquitin ligase complex that governs hnRNPK proteins stability and oncogenic functions through promoting the degradation of HnRNP K in a poly-ubiquitinaion dependent proteolysis in the prostate cancer setting. Moreover, prostate cancer-associated SPOP mutants fail to interact with and promote the destruction of hnRNPK proteins.

Conclusion

Our finding reveal new post-transcriptional and post-translational modifications mechanism of hnRNPK regulation via miR-206/ miR-613 and SPOP, respectively. More important, given the critical oncogenic role of hnRNPK and high frequency of SPOP mutation in prostate cancer, our results provide a molecular rationale for the clinical investigation of novel strategies to combat prostate cancer based on SPOP genetic status.

Background

Prostate cancer (PrCa) is one of the most prevalent malignancies among males in the western world and represents a major health concern in many industrialized countries [1]. >30% patients experience biochemical recurrence and emergence of advance-stage disease particularly, metastatic progression. The disease further progresses to castration-resistant prostate cancer (CRPC) in about 12–24 months after androgen-deprivation therapy, which still lacks an effective cure and patients rapidly progress to the incurable stage prostate cancer with mean survival time of only 16–18 months[2, 3]. Therefore, significant efforts have been devoted to better understand the mechanism of oncogenesis and to develop additional effective therapeutics targeting pivotal oncogenes, cancer-related signal transduction pathways, and epigenetic regulators [4].

hnRNP K is specific for hnRNP family members, and compared with other hnRNP proteins, has different structural characteristics (KH domain and DNA binding sites), so that it can participate in numerous cellular processes in the nucleus and cytoplasm. Of note, in addition to having the same functions with other hnRNPs it can regulate DNA transcription, pre-mRNA processing and translation, particularly with regards to the process of oncogene expression [5, 6]. All these features make it exhibit multiple roles in the cell cycle, apoptosis and tumor metastasis [7]. According to previous results, there is a close association between tumors and hnRNP K; it often shows a high expression in a variety of tumors and is closely associated with poor cancer prognosis in patients, including lung cancer, colorectal cancer, bladder cancer, hepatocelluar carcinoma and Neuroblastoma [7–11]. Ciarlo et al demonstrated that hnRNP K was strongly overexpressed in a primary human PrCa, and played a central role in the neuroendocrine differentiation regulation [12]. In addition, Wang et al have shown that a novel transcriptional repressor complex containing Pur α and hnRNP K binds to the androgen receptor (AR) gene both in cell lines and in primary human prostate tissues [13]. More recently, evidence has been provided for a role played by hnRNP K in the regulation of AR expression via a post transcriptional mechanism [14, 15]. Although hnRNPK is a critical regulator of malignancy in prostate cancer setting, its own molecular mechanism is not well evaluated, especially for its transcriptional regulation and degradation.

The deregulation of small ncRNAs, such as microRNAs (miRNAs), has been recognized as one mechanism involved in the induction and progression of PrCa. It acts either as a tumor suppressor or promoter depending on the specific targets and tumor microenvironment [16, 17]. In addition, Systematic sequencing studies revealed that recurrent somatic mutation is a key feature of prostate cancer and the most frequently mutated gene is SPOP (speckle-type POZ protein), which encodes a Cullin 3-based E3 ubiquitin ligase, with recurrent mutation in 10–15% of primary human prostate cancers[18]. SPOP has been shown to participate in diverse cellular processes and plays tumor suppressive and oncogenic roles in prostate cancer by targeting different substrates for ubiqutination-mediated proteolysis, including the androgen receptor (AR)[19], steroid receptor coactivator 3 (SRC-3)[20], DEK, TRIM24[21], BRD4[22] and Nanog[23]. Furthermore, prostate cancer-associated SPOP mutants are deficient in binding with and promoting the degradation of substrates leading to increased prostate cancer cell proliferation and

invasion, indicating the loss-of-function of SPOP mutations and the tumor suppressive role of SPOP in prostate cancer [19, 22]. Therefore, identification of additional SPOP substrates would benefit prostate cancer clinical diagnosis and therapy.

In this study, we identified that hnRNPK dysregulation in prostate carcinogenesis is correlated with a decrease in miR-206 and miR-613 expression. Further, we found that miR-206 and miR-613 inhibits hnRNPK expression by directly targeting its 3'-UTR, and thereby represses PrCa cell proliferation. Moreover, we explored oncoprotein hnRNPK as a novel ubiquitin substrate of SPOP in the prostate cancer setting, and prostate cancer-associated SPOP mutants fail to promote the degradation of hnRNPK proteins.

Materials And Methods

Patients and tissue samples

PrCa samples and adjacent normal tissue samples were collected during radical prostatectomy from PrCa patients between 2010 and 2016 at the Tongji Hospital, Tongji Medical College, Huazhong University of Science and Technology in Wuhan, China. The PrCa cases selected were based on a clear pathological diagnosis, follow-up data, and absence of androgen deprivation therapy, chemotherapy, radiotherapy or other anticancer treatment before surgery. All specimens had confirmed pathological diagnosis and were classified according to the WHO criteria. The clinicopathological patient information was collected and summarized in **Supplememt table 1.** All protocols were approved by the Ethics Committee of Tongji Hospital, Tongji Medical College, Huazhong University of Science and Technology, and informed consent was obtained from all patients before surgery. All in vivo protocols were approved by the Institutional Animal Care and Use Committee of Tongji Hospital, Tongji Medical College, Huazhong University of Science and Technology.

Bioinformatics analysis databases

The correlation of hnRNPK and SPOP expression with the biochemical recurrence of tumor patients were analyzed via Gene Expression Omnibus (https://www.ncbi.nlm.nih.gov/geo/). The miRNA target predicting algorithm TargetScan Release 7.1 (http://www.targetscan.org/vert_71/) was used to predict miRNAs targeting hnRNPK and their binding regions.

Cell culture

HEK293, HEK293T and mouse embryonic fibroblasts (MEFs) cells were maintained in Dulbecco's Modified Eagle Medium (DMEM) (Life Technologies, CA) containing 10% fetal bovine serum (FBS) (Gibico), 100 units of penicillin and 100 mg/ml streptomycin. Prostate cancer cell line PC-3, DU145, 22Rv1, C42, VCaP and LNCaP were obtained from ATCC and maintained in RPMI1640 (Life Technologies, CA) supplemented with 10% FBS. The normal prostate epithelial cells RWPE-1 (ATCC) were maintained in Keratinocyte-SFM (Gibco, GrandIsland, NY, USA). SPOP knockout and counterpart mouse embryonic fibroblasts (MEFs) were kindly offered by Dr. Wenyi Wei (Harvard Medical School, Boston, MA, USA) and

Dr. Xiangpeng Dai (Jilin University, Changchun, China) No mycoplasma contamination was observed in these cell lines. All cells were cultured in a humidified atmosphere of 5% CO2 maintained at 37˚C.

Oligonucleotide, Plasmids construction

All small RNA molecules were ordered from RiboBio Co., Ltd.(Guangzhou, China), including miR-206 mimics, miR-613 mimics, mimics negative controls (mimics-NC), miR-206 inhibitor, miR-613 mimics, inhibitor negative controls (inhibitor-NC), miRNA mimics are double-stranded RNA molecules containing the miR-206 and miR-613 sequence, while miR-206 and miR-613 inhibitors are single stranded RNA molecules containing the miR-206 and miR-613 reverse complement sequence, which can competitively bind to endogenous miR-206 and miR-613. Flag-tagged HnRNPK, KEAP1, KLHL1, PLZF and KLHL20 were purchased from Addgene. Myc-tagged Cullins, pLenti-HA-SPOP WT, Flag-tagged SPOP WT, HA-tagged SPOP-WT or deletion of MATH domain/BTB domain-SPOP constructs and His-tagged Ub as gift from Dr. Wenyi Wei (Harvard Medical School, Boston, MA, USA). HA-HnRNPK and Various SPOP mutants were generated in this study.

shRNAs and Establishment of stable cell lines

The specific shRNAs vectors (Supplementary Table S2) to deplete endogenous HnRNPK (shHnRNPK: TRCN0000295992), SPOP (shSPOP: TRCN0000139181, TRCN0000144406) and CULLIN3 (shCULLIN3: TRCN0000307983, TRCN0000073346) were purchased from Sigma-Aldrich (St louis, MO, USA). The above shRNAs were cloned into the lentiviral vector pLKO.1. pLKO.1-puro eGFP shRNA(SHC005, Sigma-Aldrich) plasmid as the shRNA control. The HEK293T cells were transfected with above pLKO.1 carrying the specific sequences, along with the packaging plasmids, psPAX2 and pMD2.G. The virus particles were generated and collected 48 h, 72h post-transfection, and then filtered with 0.45 μm filters (Millipore) and freshly used to infect cancer cells overnight in the presence of 4 μg/ml Polybrene (Sigma–Aldrich). After infection the Prostate cancer cell lines, the cells were selected with 1 μg/ml puromycin (Sigma–Aldrich) for 72 h to eliminate the uninfected cells before harvesting the whole cell lysates for the subsequent biochemical assays. Knockdown efficiency was confirmed at both mRNA and protein levels.

Antibodies and Reagents

All antibodies were used at a 1:1000 dilution in 5% non-fat milk for Immunoblot. Anti-HnRNPK antibody (A1701) and Anti-SRC(A0324)antibody were purchased from Abclonal, respectively. Anti-GAPDH (ab37168) antibody, anti-P27 (ab32034) antibody, anti-CyclinD1 (ab134175) antibody, anti-SPOP((ab192233), anti-CDK6 (ab124821) antibody and anti-Bax (ab32503) antibody were purchased from Abcam. Anti-SRC3 (2126), polyclonal anti-Myc-Tag antibody (2278) and monoclonal anti-Myc-Tag (2276) antibodies were purchased from Cell Signaling. Polyclonal anti-Flag antibody (F-2425), monoclonal anti-Flag antibody (F-3165, clone M2), anti-Vinculin antibody (V-4505), anti-Flag agarose beads (A-2220), anti-HA agarose beads (A-2095), peroxidase-conjugated anti-mouse secondary antibody (A-4416) and peroxidase-conjugated anti-rabbit secondary antibody (A-4914) were purchased from Sigma. Monoclonal anti-HA antibody (MMS-101P) was purchased from Biolegend. Anti-GFP (8371-2) antibody was purchased from Clontech. Anti- NF-κB p65 (#8242) antibody, anti-E-cadherin (#3195)

antibody, anti-Snail (#3879) antibody（CST）,anti-β-Catenin (#8580) antibody（anti-BCL-2 (#15071) antibody（anti-c-JUN (##9165) antibody（anti-c-MYC (#18583) antibody and anti-CDK4 (#12790) antibody were purchased from Cell Signaling Technology. Anti-Trim24 (sc-271266), anti-AR (N-20), anti-TRIM24/TIF1α (C-4), polyclonal anti-HA (SC-805), anti-p27 (SC-528) and anti-Nrf2 (sc-365949) were purchased from Santa Cruz Biotechnology. MG132 and cycloheximide (CHX) were purchased from Sigma–Aldrich.

Cell transfection, Lentivirus production

Cells were plated in growth medium at a density of 45–70%. The transfection was carried out using Lipofectamine RNAiMax (Invitrogen, Carlsbad, CA, USA) 24 h later according to the manufacturer's protocol. The final concentration of RNAs was 75 nM for each well. Others the transient transfections were performed using Lipofectamine 3000 (Invitrogen, Carlsbad, CA, USA) according to the manufacturer's protocol. For lentiviral-mediated overexpression of miR-206 and miR-613, the miR-206 and miR-613 sequence (pri miR-206 and pri miR-613) was cloned into H1-miRNA-CMV-GFP from GENECHEM, to generate the Lenti-miR-206 or Lenti-miR-613 construct. miR-NC (TTCTCCGAACGTGTCACGT) was cloned into the same backbone and the resulting construct Lenti-miR-NC served as a negative control. The transfection or infection efficiencies were detected by RT-qPCR.

RNA isolation and quantitative real-time PCR

Total RNA of cells was extracted with TRIzol reagent (Invitrogen, Carlsbad, CA) according to the manufacturer’s protocol. Reverse transcription of microRNA and mRNA were done using RevertAid™ First Strand cDNA Synthesis Kit (Fermentas, Vilnius, Lithuania) and miProfile™ miRNA qPCR Primer (GeneCopoeia, Guangzhou,China). RT-qPCR analysis of miRNA was performed with the Platinum SYBR Green qPCR Supermix UDG kit (Invitrogen, Carlsbad, CA) using synthesized primers from GeneCopoeia (Guangzhou, China). The U6 primers were obtained from GeneCopoeia. All experiments were done in triplicate. The expression level values were normalized to those of the small nuclear RNA U6 as a control. Several primer sequences used are listed in Supplementary Table S2.

Immunoblots and immunoprecipitation

Harvested cells washed by PBS and lysed in EBC buffer (50 mM Tris pH 7.5, 120 mM NaCl, 0.5% NP-40) supplemented with protease inhibitors (Complete Mini, Roche) and phosphatase inhibitors (phosphatase inhibitor cocktail set I and II, Calbiochem). The protein concentrations of lysates were measured by the Beckman Coulter DU-800 spectrophotometer using the BioRad protein assay reagent. Same amount of protein samples were separated by electrophoresis in sodium dodecyl sulfonate (SDS)-polyacrylamide gel and transferred onto a nitrocellulose filter (NC) membrane (Amersham). The membrane was incubated in 5% nonfat dry milk/TBST for 1 h; and then incubated with the primary antibody at 4°C overnight. The membrane was washed with TBST for three times, followed by incubated with second antibody for 1 h at room temperature. Proteins of interest were measured by electrochemiluminescence (ECL) assay. For immunoprecipitation, Cells were washed with PBS and lysed in the IP lysis buffer (25mM Tris•HCL pH7.4, 150mM NaCl, 1mM EDTA, 1% NP-40, 5% glycerol, 1 × Thermo protease inhibitor). Protein

incubated 1000μg of cell lysate with the primary antibody-conjugated beads at 4°C for 4 h. The immunocomplexes were washed 3 times with IP lysis buffer before being resolved by SDS-PAGE and immunoblotted with the indicated antibodies.

Protein half-life assays

Cells were treated with indicated condition. For half-life studies, 100 μg/ml cycloheximide (CHX, Sigma–Aldrich) was added to the cells after 36 h of post transfection. At the indicated time points, cells were harvested and protein concentrations were measured. Total 30 μg of the indicated whole cell lysates were separated by SDS-PAGE and protein levels were measured by immunoblot analysis.

In vivo ubiquitination assays

For the In vivo ubiquitination assay, 293T cells were seeded and transiently transfected with plasmids for His-Ub and other indicated proteins. Thirty-six hours after transfection, cells were treated with MG132 (20 μM) for 6 h before they were harvested. Cells were washed with PBS and lysed with IP lysis buffer (25mM Tris·HCL pH7.4, 150mM NaCl, 1mM EDTA, 1% NP-40, 5% glycerol, 1 × Thermo protease inhibitor). 1000μg of cell lysate were incubated with indicated antibody at 4°C for 4 h and then incubated with Protein A/G plus agarose overnight. Beads were washed with lysis buffer for 3 times and detected by SDS-PAGE.

Colony formation and MTS cell proliferation assay

The colony formation assay was conducted as previously described[24]. Briefly, exponentially growing cells were plated at approximately 2000 cells per well in 6-well plates after transfection. Culture medium was changed every 3 days. Colony formation was analyzed 12 days following infection by staining cells with 0.05% crystal violet solution for 30 min. The number of colonies was counted using an inverted microscope (Olympus, Japan). Cell proliferation was assessed by using the CellTiter 96 Aqueous One Solution Cell Proliferation. Assay kit (Promega, Madison, WI, USA) as previously described. Briefly, RNA transfected cells were grown in 96-well plates at a density of 2000 cells/well. Cell growth was measured daily for 4 days. At each time point, 20 μl of CellTiter 96 Aqueous One Solution was added and incubated. Absorbance was detected by a microplate reader (Bio-Rad, Berkeley, CA, USA) at 490 nm.

Cell cycle

At 72 h after transfection, cells were fixed in 70% cold ethanol, incubated with RNase A (Sigma,St. Louis, MO, USA) and stained by propidium iodide (PI) (Nanjing KeyGen Biotech Co., Ltd., Nanjing, China) staining solution. After staining, the cells were analyzed on a FACSort flow cytometer (BD Biosciences, San Diego, CA, USA). The data were processed by CELL quest software (BD Biosciences).

Luciferase reporter assay

hnRNPK 3'UTR reporter and control constructs were purchased from GENECHEM. Tumor cells overexpressing miR-206/613 and miR-NC cultured in 48-well plates were co-transfected with 1.5 mg of firefly luciferase reporter and 0.35 ng Renilla luciferase reporter with Lipofectamine RNAiMax (Invitrogen, Carlsbad, CA, USA). 24 hours post transfection, firefly luciferase activities were measured using the Dual

Luciferase Assay (Promega) and the results were normalized with Renilla luciferase according to the manufacturer's protocol.

Immunohistochemistry (IHC)

Formalin-fixed, paraffin-embedded tissue sections (5 μm) were deparaffinized in xylene and rehydrated with gradient concentrations of ethanol. The tissue sections were stained with specific antibodies against hnRNPK (1:400) (Abcam, ab32969). Sections incubated with secondary antibodies in the absence of primary antibodies were used as negative control. Hematoxylin was used for counterstaining. Slides were viewed and photographed under a light microscope.

Xenograft model of PrCa in nude mice

For mouse xenograft assay, six-week-old BALB/c-nu/nu mice were randomly divided into two or three different experimental groups. Prostate cancer cells (1×10^6) were collected and suspended in 100μl PBS mixing with Matrigel (BD 356234, 2:1) and injected into the nude mouse. Tumor onset was measured with calipers at the site of injection every 3–4 days by two trained laboratory staff members at different times on the same day, starting 12 days after injection when appreciable tumor formed subcutaneously. Tumor volume was calculated using the formula, $V = 0.5ab^2$, where a represents the larger and b represents the smaller of the two perpendicular indexes. Animals were euthanized and xenografts were harvested 40 days after injection and tumors were weighed, and target gene expression were evaluated. Nude mice were manipulated and cared for according to NIH Animal Care and Use Committee guidelines in the Experiment Animal Center of the Tongji Medical College of Huazhong University of Science and Technology, China.

Statistical analysis

GraphPad Prism 8 was used for analysis. The differences between two groups or more than two groups were compared using Student's t-test. Survival analyses were conducted by Kaplan-Meier curve and log-rank test. The linear regression test was used to analyze the genes expression correlation. $P < 0.05$ was regarded as statistically significant. All the data are showed as mean ± SD.

Results

hnRNP K is frequently overexpressed in prostate tissues and cell lines

To detect hnRNPK protein levels in prostate cancer, we first performed IHC analysis on 22 primary prostate adenocarcinoma. We found that hnRNPK was mainly located in the nucleus of PrCa cells, and it levels were high in 13 cases (59.1%). Moreover, hnRNPK expression was obviously higher in intermediate/high-risk tissues as compared to low-risk tissues (Fig. 1A). Further, we analyzed hnRNPK expression in lysates from 27 freshly harvested tissue samples of PrCa patients by Immunoblotting compared with matched noncancerous tissues. Among 27 randomly selected PrCa and paired

noncancerous prostate tissues, 15 tumors (55.6%) showed an increase in hnRNPK protein (Fig. 1B). Moreover, we detected hnRNPK mRNA expression in 53 paired PrCa tissues and its levels were significantly higher than adjacent noncancerous prostate tissues (Fig. 1C). Additionally, a public data set (Gene Expression Omnibus, GSE70770) containing 35 PrCa tissues and 14 normal prostate tissues also showed that hnRNPK mRNA expression was upregulated in PrCa tissues (Fig. 1D). To further investigate the clinicopathological and prognostic significance of hnRNPK levels in PrCa patients, the mRNA levels of hnRNPK in above cohort of 53 PrCa tissues in which absence of androgen deprivation therapy, chemotherapy, radiotherapy or other anticancer treatment before surgery were classified according to age, Serum PSA, Gleason score, pT stage, Lymph node metastasis, Seminal vesicle invasion and Biochemical recurrence. We found that high hnRNPK mRNA expression was significantly associated with higher PSA levels and biochemical recurrence (P<0.05, Supplement Table 1). This prognostic value was also confirmed using a larger cohort of 203 PrCa patients retrieved from the GSE70770 database, high expression of hnRNPK was associated with higher biochemical recurrence rates (P<0.05, Fig. 1E). As shown in Fig. 1F and G, hnRNPK mRNA and protein expression were remarkably high in C4-2, DU145 and PC-3 cell lines compared with the normal prostate epithelial cells RWPE-1 or other PrCa cell lines. Thus, hnRNPK expression was frequently higher in PrCa tissues and cell lines than in the normal ones, which predicted poor prognosis in PrCa patients.

Knockdown of hnRNPK inhibits cell growth and cell cycle progression of prostate cells

To determine the biological functions for hnRNPK, we firstly performed loss-of-function experiments and knocked down hnRNPK by using short hairpin RNAs (shRNAs) in PC-3 and DU145 cells, respectively. The efficiency of knockdown were confirmed by mRNA and protein levels with RT-qPCR and Immunoblots (Supplement Fig. 1). The results of MTS assay showed that the proliferation capacity of PC-3 and DU145 cells was significantly reduced after silencing of hnRNPK experssion (Fig. 2A and 2B). Colony formation assays further confirmed significantly inhibited of cellular growth in both PrCa cells line following hnRNPK silencing (Fig. 2C and D). Moreover, Flow cytometry results indicated that the proportion of cells in the G0/G1 phase was significantly higher and the proportion of cells in the S phase was significantly lower in hnRNPK-silenced cells than in the control cells (Fig. 2E and F). Consistently, control sh-NC DU145 cells and the corresponding stable hnRNPK-silenced cells were inoculated into BALB/C athymic mice. As shown in Fig. 2G and H, tumors formed by the hnRNPK-silenced cells were retarded in size and weight than those formed from the control cells. Then the relative expression of hnRNPK in xenograft tumor tissue were verified by RT-qPCR (Fig. 2I). Collectively, these results indicate that hnRNPK inhibits PrCa cell proliferation in vitro and vivo via its effects on the cell cycle and may play oncogenic roles in prostate cancer progression.

miR-206 and miR-613 expression are downregulated in prostate tissues and cell lines and directly targets hnRNPK

Among the 53 randomly selected paired tissues from primary PrCa patients (Same cases above-mentioned), miR-206 and miR-613 expression were found to be reduced in tumor tissues when compared with paired noncancerous tissues (Fig. 3A and 3C), which further confirmed by using two public datasets, GSE21036 and GSE60117, respectively (Fig. 3B and 3D). Moreover, we analyzed miR-206 and miR-613 mRNA expression in six PrCa cell lines and found that miR-206 in C4-2, VCap, PC-3 and DU145 cell lines (Fig. 3E) and miR-613 in C4-2, LNCap, PC-3 and DU145 cell lines (Fig. 3F) had lower levels than in the normal prostatic cell line RWPE-1. Further we used TargetScan7.1 algorithms, a bioinformatic tool for microRNA target prediction to identify additional novel targets of miR-206 and miR-613, and found both of them could bind to the 3’-UTR of hnRNPK mRNA(Fig. 3G and 3H). Therefore, it is possible that both of miRNA inhibits hnRNPK expression in PrCa tissues and cell lines by directly binding to its 3’-UTR region. By employed a dual-luciferase reporter system, we subcloned 3’-UTR of hnRNPK mRNA including the predicted miR-206 and miR-613 recognition site (Wt) or the mutated sequences (Mut) into the pGL3 vector, downstream of the luciferase open reading frame. miR-LacZ as a miRNA blank vector control. Obviously, miR-206 and miR-613 inhibited the activity of luciferase with the wild-type but not mutant 3’-UTR of hnRNPK in DU145 cells, respectively (Fig. 3I). We further identified that whether miR-206 or miR-613 negatively regulated the expression of hnRNPK in PrCa. Our data firstly confirmed that the efficiency of overexpression and knockdown for miR-206 and miR-613 in PrCa cells which transfected with their corresponding mimics or inhibitor, respectively. (Supplement Fig. 2). Then, in line with the expression of miR-206 and miR-613, the level of hnRNPK showed a tendency toward an inverse correlation as determined by using RT-qPCR and Immunoblot analysis (Fig. 3J-3L). Taken together, these data support the bioinformatic prediction suggesting the 3’-UTR of hnRNPK is a direct target of miR-206 and miR-613.

Overexpression of miR-206/miR-613 can inhibit PrCa cell proliferation in vitro and vivo

Next, we sought to understand the biological effects of miR-206 and miR-613 in Prostate cancer, we induced overexpression of miR-206/miR-613 by using of miR-206/miR-613 mimics and silencing of miR-206/miR-613 using the of miR-206/miR-613 inhibitor in PrCa cells and studied the effects on cell growth. CCK-8 and colony formation assays showed that PrCa cells overexpressing miR-206 or miR-613 had significantly lower proliferation ability than the control cells (Fig. 5A and 5C). In contrast, silencing of endogenous miR-206 or miR-613 led to a significantly higher proliferation rate than observed in the control cells, with the exception of the PC-3 cell lines (Fig. 5B and 5D). Next, Flow cytometry results indicated overexpressing miR-206 or miR-613 dramatically increased the cell population in the G0/G1 phase, whereas it reduced the cell population in the S and G2/M phases (Fig. 5E). On the contrary, depletion of endogenous miR-206 or miR-613 decreased the cell population in the G0/G1 phase and increased the cell population in the S and G2/M phases in DU145 cells (Fig. 5F). Consistently, induction

of miR-206 or miR-613 by shRNA in DU145 cells significantly retarded tumor growth in xenograft mouse models (Fig. 5G and 5H). Then the relative expression of hnRNPK, miR-206 and miR-613 in tumor tissue were verified by RT-qPCR (Fig. 5I-K). Taken together, miR-206 or miR-613 could exert a significant inhibitory effect on tumorigenesis by repressing hnRNPK in vitro and vivo.

In line with the results for hnRNPK-silenced cells mediated by miR-206 or miR-613, the protein abundance of Cycle D1, CDK4, CDK6, which promote the cell cycle, were significantly decreased, whereas the protein abundance of P27, which arrests the cell cycle, was obviously increased than in the control cells. Moreover, depletion of endogenous hnRNPK significantly up-regulated the protein levels of apoptosis, such as that for BAX, NF-Kb/p65, c-JUN, and inhibited the anti-apoptotic protein levels for BCL-2 and oncogenes c-MYC. Interestingly, hnRNPK-silenced cells also exhibited increased protein abundance of the transcription factor Snail and oncogenes c-SRC, decreased the biomarkers of EMT, such as E-cadherin and β catenin(Fig. 5L). On the contrary, hnRNPK-upregulated cells mediated by miR-206 or miR-613 inhibitor showed an inverse tendency for above mentioned proteins abundance (Fig. 5M). The correlation network dataset (GSE 88808) also indicated that hnRNPK shared similar correlation with above mentioned proteins (Supplement Fig. 3). These data strongly suggest that hnRNPK regulates several biological functions crucial for prostate cancer development, including proliferation, apoptosis and EMT.

$Cul3^{SPOP}$ E3 ligase degrades hnRNP K protein

Above findings have revealed a new post-transcriptional mechanism of hnRNPK regulation via miR-206 and miR-613 and thereby represses prostate cancer cell proliferation. Interestingly, with the results for hnRNPK-silenced prostate cancer cells mediated by miR-206 and miR-613, led to higher SPOP expression than in the control cells (Fig. 5A). In addition, the SPOP mRNA expression in the correlation network dataset (GSE 88808) also showed a tendency toward a strongly inverse correlation with hnRNPK in PrCa (Supplement Fig. 3). Two public datasets further confirmed that SPOP mRNA expression was significantly downregulated in human prostate cancer tissues (GSE60329) (P<0.05, Fig. 5B) and low expression of SPOP was associated with higher biochemical recurrence rates (GSE46602) (P<0.05, Fig. 5C).

SPOP, a Cullin 3-based E3 ubiquitin ligase, has been shown to participate in diverse cellular processes and plays tumor suppressive and oncogenic roles in prostate cancer[20, 22], suggested Cullin-Ring family E3 ligase(s) may be the upstream regulator(s) to control hnRNPK protein stability. To uncover the underlying regulatory mechanisms, we firstly screened a panel of Cullin scaffolding proteins to identify the potential E3 complex for HnRNPK. Cullin 3, and to a much lesser extent, Cullin 4A, but not other Cullin family members specifically interacted with HnRNPK in cells (Fig. 5D). In keeping with this notion, deletion of endogenous Cullin 3 in Prostate cancer cell lines including C4-2 and 22Rv1, could dramatically upregulate the protein abundance of endogenous HnRNPK (Fig. 5E and 5F). Previous studies demonstrated that Cullin 3 recruits downstream ubiquitin substrates through interaction with BTB-domain-containing proteins as substrate-specific adaptors, including but not limited to SPOP, KEAP1,

KLHL1, PLZF and KLHL12[25]. However, we found that only SPOP, but not other Cullin 3-based BTB-domain-containing adaptor proteins we examined, specifically interacts with HnRNPK(Fig. 5G). Notably, SPOP promoted HnRNPK degradation in a dose-dependent manner in prostate cancer cell (Fig. 5H). More importantly, SPOP-mediated degradation of HnRNPK could be efficiently blocked by MG132 (Fig. 5I), indicating that SPOP regulates HnRNPK abundance through the ubiquitin-proteasome pathway. Consistent with these findings, depletion of endogenous SPOP by shRNAs or CRISPR-mediated knockout in multiple human prostate cancer cell lines or MEFs led to a marked increase in the protein abundance of HnRNPK as well as other identified SPOP substrates, including TRIM24, SRC3, AR and DEK (Fig. 5J-N). Moreover, we found that SPOP, but not KEAP1, another Cullin 3-based adaptor protein we examined, specifically promotes HnRNPK ubiquitination in cells (Fig. 5O). And subsequently the half-life of HnRNPK was significantly extended in SPOP -depleted cells (Fig. 5P and 5Q). Our results collectively suggest that the HnRNPK is potential downstream substrates of the Cullin 3 SPOP E3 ubiquitin ligase.

Patients-associated SPOP mutants are incapable to degrade HnRNPK

SPOP is a member of the MATH-BTB protein family containing an N-terminal MATH domain and a C-terminal BTB domain [25]. The MATH domain is responsible for substrate recognition and interaction, while the BTB domain binds Cullin 3 forming the functional E3 ubiquitin ligase complex. Recent genome-wide sequencing studies have revealed that SPOP, as the major frequently mutated gene in prostate cancer, plays pivotal roles for prostate tumorigenesis and metastasis. Interestingly, Most of the somatic mutations identified in prostate cancers such as Y87C, F102C, W131G and F133V, occurred in MATH domain and play a dominant-negative role in substrate binding and degradation (Fig. 6A). In keeping with previous reports [18, 21], we found that deletion of the MATH domain abolishes SPOP interaction with HnRNPK (Fig. 6B) and both the MATH domain and BTB domain are required for SPOP-mediated HnRNPK ubiquitination and degradation (Fig. 6C). Consistently, we sought to explore whether prostate cancer-associated SPOP mutations affect HnRNPK stability. Conceivably, prostate cancer patients-associated SPOP mutants W131G and F102C failed to interact with (Fig. 6D), and were thereby deficient in promoting the degradation of HnRNPK (Fig. 6E). Moreover, ectopic expression of SPOP-WT, but not the SPOP mutants, significantly shortened the half-life of HnRNPK (Fig. 6F and 6G) and promoted HnRNPK ubiquitination in cells (Fig. 6H). These data indicate that patient-associated SPOP mutants are deficient in promoting ubiquitination and destruction of HnRNPK, therefore partially providing a molecular mechanism to explain the aberrant accumulation of HnRNPK in prostate cancer tissue.

Disscussion

It is our novel discovery that highlight the oncogenic role of hnRNPK in PrCa and miR-206 or miR-613 inhibits hnRNPK expression at post-transcriptional level by directly targeting hnRNPK 3’-UTR and thereby represses PrCa cell carcinogenesis. This miRNA-mediated downregulation of hnRNPK provides new insight into therapy strategies for PrCa. On the other hand, our studies delineated the upstream post-

translationally regulatory mechanisms of hnRNPK by SPOP-mediated poly-ubiquitination and subsequent degradation in prostate cancer. Hence, we envision that our studies will provide the rationale for developing optimal treatment strategy based on individual tumor genetic status for individual prostate cancer patient.

Post-transcriptional gene regulation (PTGR) is involved in the precise control of many oncogenes and tumor-suppressing genes. As the trans-acting factors and tumor suppressors or oncogenes, miRNAs have key roles in PTGR mainly through interactions with the 3'-UTR of target mRNAs in various human cancers (cis-elements)[26]. In this study, we focused on PrCa cells and tissues to determine whether miRNAs can epigenetically influence hnRNPK expression. Intriguingly, the expression of miR-206 and miR-613 was downregulated and inversely correlated with hnRNPK expression in the PrCa tissues and in majority of prostate cancer cell lines, implying that miR-206 and miR-613 might functionally contributes to the expression of hnRNPK in PrCa. Therefore, we performed in silico prediction of microRNA targets and found that miR-206 and miR-613 can both potentially bind to target sites of hnRNPK 3'-UTR. Then, we used luciferase reporter assay to confirm that hnRNPK is a bona fide target of miR-206 and miR-613 which negatively regulates the expression of hnRNPK at post-transcriptional level. In functional studies, we assessed the effect of miR-206/miR-613 and hnRNPK on PrCa growth both in vitro and in vivo. miR-206/ miR-613 overexpression significantly repressed proliferation and colony formation of tumor cells in vitro. These effects appeared to be mediated by inhibition of hnRNPK oncogene, leading to an arrest of tumor cells at G1 phase of the cell cycle. Furthermore, transfection of miR-206/ miR-613 suppressed effectively tumorigenicity of PrCa cells in a nude mouse model. Supporting our findings, recent studies have found that hnRNPK down-regulation suppressed cell proliferation in pancreatic cancer [27]. But the underlying mechanism remains largely unknown. We further determined that hnRNPK regulates the cell cycle of prostate cancer cells mainly by transcriptional regulation of Cycle D1, CDK4, CDK6 and P27. In addition, we first demonstrated that hnRNPK maintained anti-apoptosis in prostate cancer cells via transcriptional regulation of BAX, NF-Kb/p65, c-JUN and BCL-2. Similarly, hnRNPK suppresses apoptosis independent of p53 status in hepatocellular carcinoma by increasing XIAP transcription[28], suggesting that the mechanism of hnRNPK on apoptosis differs between cancers. Moreover, newly studies have found that hnRNPK transcription and translation activates several important oncogenes, including c-MYC[6, 29], and inhibits its interaction with c-Src[30]. Consistent with our findings, c-MYC was activated, whereas c-SRC was inhibited via downregulated miR-206/613 in prostate cancer cell. These results suggest that hnRNPK plays an oncogenic role in prostate cancer by directly mediating these genes. Interestingly, hnRNPK silencing led to lower E-cadherin and β catenin and higher Snail expression, which theoretically can promote EMT for PrCa cell and prompt us to further elucidate the function of hnRNPK in EMT.

HnRNPK is subject to several post-translational modifications, such as methylation[31] and sumoylation[32], which can regulate its interactions with different molecules and influence its functions. However, the ubiquitination and degradation of HnRNPK in normal condition or other tissue context, especially in prostate cancer are not well investigated. We firstly provide experimental evidence demonstrating that the E3 ubiquitin ligase SPOP plays a critical tumor suppressive role in prostate cancer

by specifically binding and promoting the degradation of HnRNPK in a poly-ubiquitinaion. Interestingly, Previous studies have reported that hnRNPK was stabilized following DNA damage through the inhibition of its HDM2-mediated ubiquitin-dependent degradation in SAOS2 and U2OS cells[33]. However, induction of hnRNPK in response to DNA damage and ubiquitylation of hnRNPK mediated by wild-type HDM2 was not generally seen in all panel of cancer cell lines, suggested that it is plausible each E3 ligase is working in different cell and cell cycle phase, or in a temporal or spatial specificity to provide a timely control of the hnRNPK stability.

Although prostate cancer has been associated with a low mutational burden, one of the most common recurrently mutated genes in this tumor is Cullin3^{SPOP}[18, 34]. SPOP protein play a role as a tumor suppressor that negatively regulates the multiple other oncogenic substrates stability in PrCa, including AR, SRC-3, c-MYC, ERG, DEK, BRD4 and Trim24 [19–22, 35–37]. It mutations has been identified as early and divergent driver events in prostate carcinogenesis. Notably, our results showed that prostate cancer-associated SPOP mutants including F102C and W131G, which are clustered in its substrate-recruiting MATH domain, restrain its capability to bind and promote hnRNPK poly-ubiquitination and degradation. Thus, our current study provides a possible mechanism to explain why hnRNPK overexpressed in Prostate cancer, in part by evading SPOP-mediated degradation. However, many more studies are warranted in future such as identify specific degron of HnRNPK as the major motif that is responsible for SPOP-dependent regulation of its stability. Moreover, consistent with a critical role for HnRNPK to serve as transcriptional co-activator for AR, it is worthwhile investigating that the AR target genes, and AR inhibitor sensitivity correlate with hnRNPK overexpressed in somatic SPOP mutations cells.

Conclusions

In summary, it is our novel discovery that highlight the oncogenic role of hnRNPK in PrCa and miR-206 or miR-613 inhibits hnRNPK expression at post-transcriptional level by directly targeting hnRNPK 3’-UTR and thereby represses PrCa cell carcinogenesis. This miRNA-mediated downregulation of hnRNPK provides new insight into therapy strategies for PrCa. On the other hand, our studies delineated the upstream post-translationally regulatory mechanisms of hnRNPK by SPOP-mediated poly-ubiquitination and subsequent degradation in prostate cancer. Hence, we envision that our studies will provide the rationale for developing optimal treatment strategy based on individual tumor genetic status for individual prostate cancer patient.

Abbreviations

miR-206, microRNA-206, miR-613, microRNA-613, PrCa, prostate cancer, 3’-UTR, 3’-untranslated region, hnRNPK, Heterogeneous nuclear ribonucleoprotein K, AR androgen receptor, CRPC, castration-resistant prostate cancer, SPOP, speckle-type POZ protein, SRC-3, steroid receptor coactivator 3, TRIM24, Tripartite motif-containing 24, shRNAs, short hairpin RNAs, PTGR, Post-transcriptional gene regulation, CDK6, cyclin dependent kinase 6, CDK4, cyclin dependent kinase 4, EMT, epithelial-mesenchymal transition, MEFs, mouse embryonic fibroblasts, CHX ,cycloheximide.

Declarations

Acknowledgements

We would like to express our gratitude to all those who financed the subject. We thank Xiangpeng Dai for critical reading of the manuscript and helpful discussions, This study was supported by the National Natural Science Foundation of China [grant number 81772729, 81302218].

Funding

This study was supported by the National Natural Science Foundation of China [grant number 81772729, 81302218].

Contributions

H.J., W.H.L. and L.S.M. designed and performed most of the experiments. H.J., W.H.L. wrote the main manuscript text. Y.Z.Q. and W.S.G modified the manuscript. H.J., Y.C.H. and L.S.M. prepared the figures and tables. W.H.L., Q.D.X., P.Z., X.M.L.,X.Y. and L.S.M. carried out experiments and analyzed the data. All authors discussed the results and commented on the manuscript.

Availability of data and materials

All data generated during this study are included in this article.

Competing financial interests

The authors declare no potential conflicts of interest with respect to the authorship and/or publication of this article.

Ethics approval and consent to participate

All protocols were approved by the Ethics Committee of Tongji Hospital, Tongji Medical College, Huazhong University of Science and Technology, and informed consent was obtained from all patients before surgery.

Consent for publication

Not applicable.

References

1. Kelly SP, Rosenberg PS, Anderson WF, Andreotti G, Younes N, Cleary SD, Cook MB: **Trends in the Incidence of Fatal Prostate Cancer in the United States by Race.** *Eur Urol* 2017, **71:**195-201.
2. Karantanos T, Corn PG, Thompson TC: **Prostate cancer progression after androgen deprivation therapy: mechanisms of castrate resistance and novel therapeutic approaches.** *Oncogene* 2013,

32:5501-5511.

3. Damodaran S, Lang JM, Jarrard DF: **Targeting Metastatic Hormone Sensitive Prostate Cancer: Chemohormonal Therapy and New Combinatorial Approaches.** *J Urol* 2019, **201:**876-885.
4. Sinha A, Huang V, Livingstone J, Wang J, Fox NS, Kurganovs N, Ignatchenko V, Fritsch K, Donmez N, Heisler LE, et al: **The Proteogenomic Landscape of Curable Prostate Cancer.** *Cancer Cell* 2019, **35:**414-427 e416.
5. Lu J, Gao FH: **Role and molecular mechanism of heterogeneous nuclear ribonucleoprotein K in tumor development and progression.** *Biomed Rep* 2016, **4:**657-663.
6. Gallardo M, Malaney P, Aitken MJL, Zhang X, Link TM, Shah V, Alybayev S, Wu MH, Pageon LR, Ma H, et al: **Uncovering the Role of RNA-Binding Protein hnRNP K in B-Cell Lymphomas.** *J Natl Cancer Inst* 2020, **112:**95-106.
7. Li D, Wang X, Mei H, Fang E, Ye L, Song H, Yang F, Li H, Huang K, Zheng L, Tong Q: **Long Noncoding RNA pancEts-1 Promotes Neuroblastoma Progression through hnRNPK-Mediated beta-Catenin Stabilization.** *Cancer Res* 2018, **78:**1169-1183.
8. Pino I, Pio R, Toledo G, Zabalegui N, Vicent S, Rey N, Lozano MD, Torre W, Garcia-Foncillas J, Montuenga LM: **Altered patterns of expression of members of the heterogeneous nuclear ribonucleoprotein (hnRNP) family in lung cancer.** *Lung Cancer* 2003, **41:**131-143.
9. Hong X, Song R, Song H, Zheng T, Wang J, Liang Y, Qi S, Lu Z, Song X, Jiang H, et al: **PTEN antagonises Tcl1/hnRNPK-mediated G6PD pre-mRNA splicing which contributes to hepatocarcinogenesis.** *Gut* 2014, **63:**1635-1647.
10. Shin CH, Lee H, Kim HR, Choi KH, Joung JG, Kim HH: **Regulation of PLK1 through competition between hnRNPK, miR-149-3p and miR-193b-5p.** *Cell Death Differ* 2017, **24:**1861-1871.
11. Chen X, Gu P, Xie R, Han J, Liu H, Wang B, Xie W, Xie W, Zhong G, Chen C, et al: **Heterogeneous nuclear ribonucleoprotein K is associated with poor prognosis and regulates proliferation and apoptosis in bladder cancer.** *J Cell Mol Med* 2017, **21:**1266-1279.
12. Ciarlo M, Benelli R, Barbieri O, Minghelli S, Barboro P, Balbi C, Ferrari N: **Regulation of neuroendocrine differentiation by AKT/hnRNPK/AR/beta-catenin signaling in prostate cancer cells.** *Int J Cancer* 2012, **131:**582-590.
13. Wang LG, Johnson EM, Kinoshita Y, Babb JS, Buckley MT, Liebes LF, Melamed J, Liu XM, Kurek R, Ossowski L, Ferrari AC: **Androgen receptor overexpression in prostate cancer linked to Pur alpha loss from a novel repressor complex.** *Cancer Res* 2008, **68:**2678-2688.
14. Mukhopadhyay NK, Kim J, Cinar B, Ramachandran A, Hager MH, Di Vizio D, Adam RM, Rubin MA, Raychaudhuri P, De Benedetti A, Freeman MR: **Heterogeneous nuclear ribonucleoprotein K is a novel regulator of androgen receptor translation.** *Cancer Res* 2009, **69:**2210-2218.
15. Gu P, Chen X, Xie R, Xie W, Huang L, Dong W, Han J, Liu X, Shen J, Huang J, Lin T: **A novel AR translational regulator lncRNA LBCS inhibits castration resistance of prostate cancer.** *Mol Cancer* 2019, **18:**109.

16. Zhang B, Pan X, Cobb GP, Anderson TA: **microRNAs as oncogenes and tumor suppressors.** *Dev Biol* 2007, **302:**1-12.
17. Rupaimoole R, Calin GA, Lopez-Berestein G, Sood AK: **miRNA Deregulation in Cancer Cells and the Tumor Microenvironment.** *Cancer Discov* 2016, **6:**235-246.
18. Barbieri CE, Baca SC, Lawrence MS, Demichelis F, Blattner M, Theurillat JP, White TA, Stojanov P, Van Allen E, Stransky N, et al: **Exome sequencing identifies recurrent SPOP, FOXA1 and MED12 mutations in prostate cancer.** *Nat Genet* 2012, **44:**685-689.
19. Geng C, Rajapakshe K, Shah SS, Shou J, Eedunuri VK, Foley C, Fiskus W, Rajendran M, Chew SA, Zimmermann M, et al: **Androgen receptor is the key transcriptional mediator of the tumor suppressor SPOP in prostate cancer.** *Cancer Res* 2014, **74:**5631-5643.
20. Geng C, He B, Xu L, Barbieri CE, Eedunuri VK, Chew SA, Zimmermann M, Bond R, Shou J, Li C, et al: **Prostate cancer-associated mutations in speckle-type POZ protein (SPOP) regulate steroid receptor coactivator 3 protein turnover.** *Proc Natl Acad Sci U S A* 2013, **110:**6997-7002.
21. Theurillat JP, Udeshi ND, Errington WJ, Svinkina T, Baca SC, Pop M, Wild PJ, Blattner M, Groner AC, Rubin MA, et al: **Prostate cancer. Ubiquitylome analysis identifies dysregulation of effector substrates in SPOP-mutant prostate cancer.** *Science* 2014, **346:**85-89.
22. Dai X, Gan W, Li X, Wang S, Zhang W, Huang L, Liu S, Zhong Q, Guo J, Zhang J, et al: **Prostate cancer-associated SPOP mutations confer resistance to BET inhibitors through stabilization of BRD4.** *Nat Med* 2017, **23:**1063-1071.
23. Zhang J, Chen M, Zhu Y, Dai X, Dang F, Ren J, Ren S, Shulga YV, Beca F, Gan W, et al: **SPOP Promotes Nanog Destruction to Suppress Stem Cell Traits and Prostate Cancer Progression.** *Dev Cell* 2019, **48:**329-344 e325.
24. Li SM, Wu HL, Yu X, Tang K, Wang SG, Ye ZQ, Hu J: **The putative tumour suppressor miR-1-3p modulates prostate cancer cell aggressiveness by repressing E2F5 and PFTK1.** *J Exp Clin Cancer Res* 2018, **37:**219.
25. Canning P, Cooper CD, Krojer T, Murray JW, Pike AC, Chaikuad A, Keates T, Thangaratnarajah C, Hojzan V, Ayinampudi V, et al: **Structural basis for Cul3 protein assembly with the BTB-Kelch family of E3 ubiquitin ligases.** *J Biol Chem* 2013, **288:**7803-7814.
26. Lin S, Gregory RI: **MicroRNA biogenesis pathways in cancer.** *Nat Rev Cancer* 2015, **15:**321-333.
27. Zhou R, Shanas R, Nelson MA, Bhattacharyya A, Shi J: **Increased expression of the heterogeneous nuclear ribonucleoprotein K in pancreatic cancer and its association with the mutant p53.** *Int J Cancer* 2010, **126:**395-404.
28. Xiao Z, Ko HL, Goh EH, Wang B, Ren EC: **hnRNP K suppresses apoptosis independent of p53 status by maintaining high levels of endogenous caspase inhibitors.** *Carcinogenesis* 2013, **34:**1458-1467.
29. Cai Z, Cao C, Ji L, Ye R, Wang D, Xia C, Wang S, Du Z, Hu N, Yu X, et al: **RIC-seq for global in situ profiling of RNA-RNA spatial interactions.** *Nature* 2020, **582:**432-437.
30. Ostareck-Lederer A, Ostareck DH, Rucknagel KP, Schierhorn A, Moritz B, Huttelmaier S, Flach N, Handoko L, Wahle E: **Asymmetric arginine dimethylation of heterogeneous nuclear ribonucleoprotein**

K by protein-arginine methyltransferase 1 inhibits its interaction with c-Src. *J Biol Chem* 2006, **281:**11115-11125.

31. Chen Y, Zhou X, Liu N, Wang C, Zhang L, Mo W, Hu G: **Arginine methylation of hnRNP K enhances p53 transcriptional activity.** *FEBS Lett* 2008, **582:**1761-1765.
32. Lee SW, Lee MH, Park JH, Kang SH, Yoo HM, Ka SH, Oh YM, Jeon YJ, Chung CH: **SUMOylation of hnRNP-K is required for p53-mediated cell-cycle arrest in response to DNA damage.** *EMBO J* 2012, **31:**4441-4452.
33. Moumen A, Masterson P, O'Connor MJ, Jackson SP: **hnRNP K: an HDM2 target and transcriptional coactivator of p53 in response to DNA damage.** *Cell* 2005, **123:**1065-1078.
34. Cancer Genome Atlas Research N: **The Molecular Taxonomy of Primary Prostate Cancer.** *Cell* 2015, **163:**1011-1025.
35. Groner AC, Cato L, de Tribolet-Hardy J, Bernasocchi T, Janouskova H, Melchers D, Houtman R, Cato ACB, Tschopp P, Gu L, et al: **TRIM24 Is an Oncogenic Transcriptional Activator in Prostate Cancer.** *Cancer Cell* 2016, **29:**846-858.
36. Geng C, Kaochar S, Li M, Rajapakshe K, Fiskus W, Dong J, Foley C, Dong B, Zhang L, Kwon OJ, et al: **SPOP regulates prostate epithelial cell proliferation and promotes ubiquitination and turnover of c-MYC oncoprotein.** *Oncogene* 2017, **36:**4767-4777.
37. Gan W, Dai X, Lunardi A, Li Z, Inuzuka H, Liu P, Varmeh S, Zhang J, Cheng L, Sun Y, et al: **SPOP Promotes Ubiquitination and Degradation of the ERG Oncoprotein to Suppress Prostate Cancer Progression.** *Mol Cell* 2015, **59:**917-930.

Figures

Figure 1

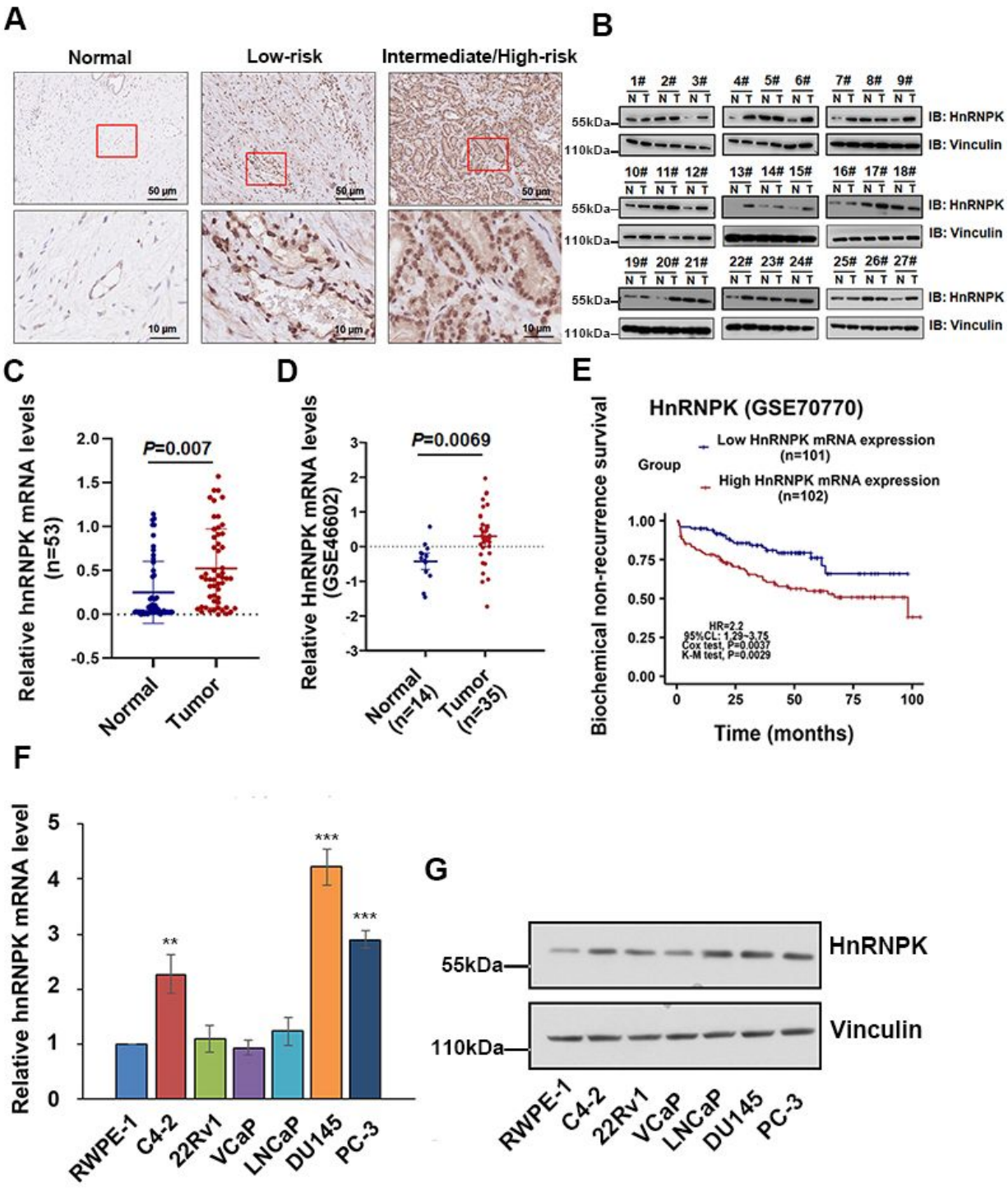

Figure 1

hnRNPK is frequently overexpressed in Prostate cancer. (A) Twenty-two formalin-fixed and paraffin-embedded primary prostate cancer tissues were subjected to IHC analyses of the hnRNPK protein. Representative images are shown in normal, low-risk, and intermediate/high-risk prostate cancer tissues, respectively. Magnification: × 400 (top) and× 1000 (bottom). (B) Immunoblot analysis of the hnRNPK protein levels in 27 randomly selected PrCa tissues and paired noncancerous prostate tissues, Vinculin

was used as an internal control. (C) hnRNPK mRNA levels in 53 PrCa tissues and paired noncancerous prostate tissues. GAPDH served as loading controls. (D) Relative hnRNPK mRNA expression levels in PrCa tissues and adjacent normal prostate tissues in a public data set (GSE70770). (E) Effect of the hnRNPK expression level on Biochemical recurrence in 203 prostate cancer patients who did not undergo androgen deprivation therapy, chemotherapy, radiotherapy or other anticancer treatment was analyzed, and Kaplan-Meier plots were generated using a Kaplan-Meier Plotter. (F) The level of hnRNPK in human prostate cancer cells was detected by RT-qPCR and Immunoblot (G), respectively. *P<0.05, **P<0.01, ***P<0.001.

Figure 2

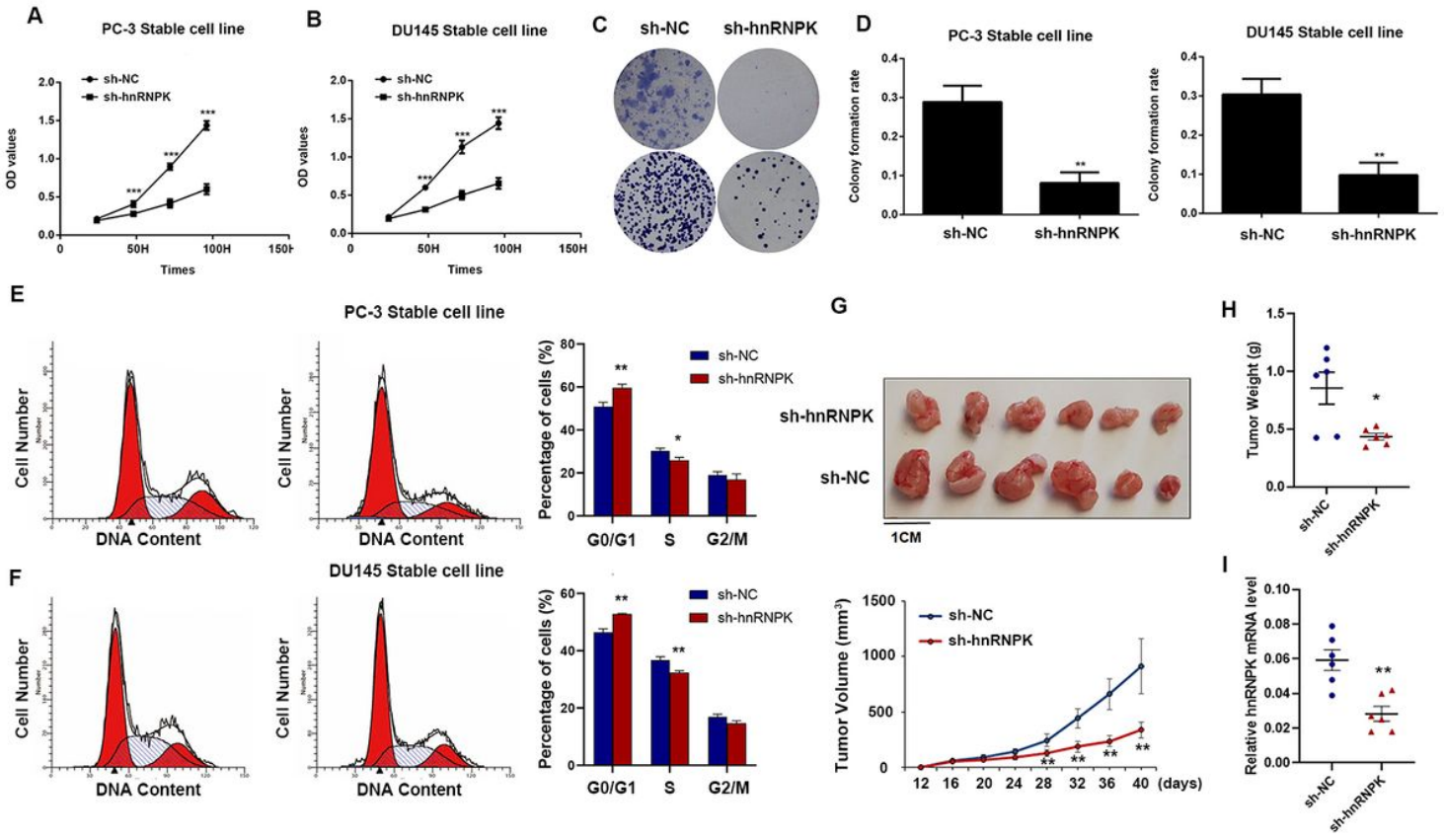

Figure 2

Knockdown of hnRNPK inhibits cell growth and cell cycle in vitro and in vivo Knocked down hnRNPK respectively by using shRNAs in PC-3 and DU145 cells. (A and B) MTS assays revealed cell viability curves of both stable PrCa cells in every 24h. (C) Representative micrographs and (D) relative quantification of crystal violet-stained cell colonies analyzed by clongenic formation. (E and F) Flow cytometric analysis of PrCa cell lines (hnRNPK-silenced cells vs. NC cells). Cells were harvested at 72 h after transfection and stained with propidium iodide. The percentage of cells in each cell cycle phase is shown in the inset of each panel. (G) hnRNPK-silenced DU145 cell xenografts in nude mice (n=6) at the experimental endpoint, tumors were dissected and photographed as shown. Tumor growth curves in mice inoculated with the indicated cells at the indicated days. (H) Each tumor formed was weighed. (I) hnRNPK

mRNA expression in tumors was detected by qRT-PCR analysis. Results were plotted as the mean ± S.D of three independent experiments. *P<0.05, **P<0.01, ***P<0.001.

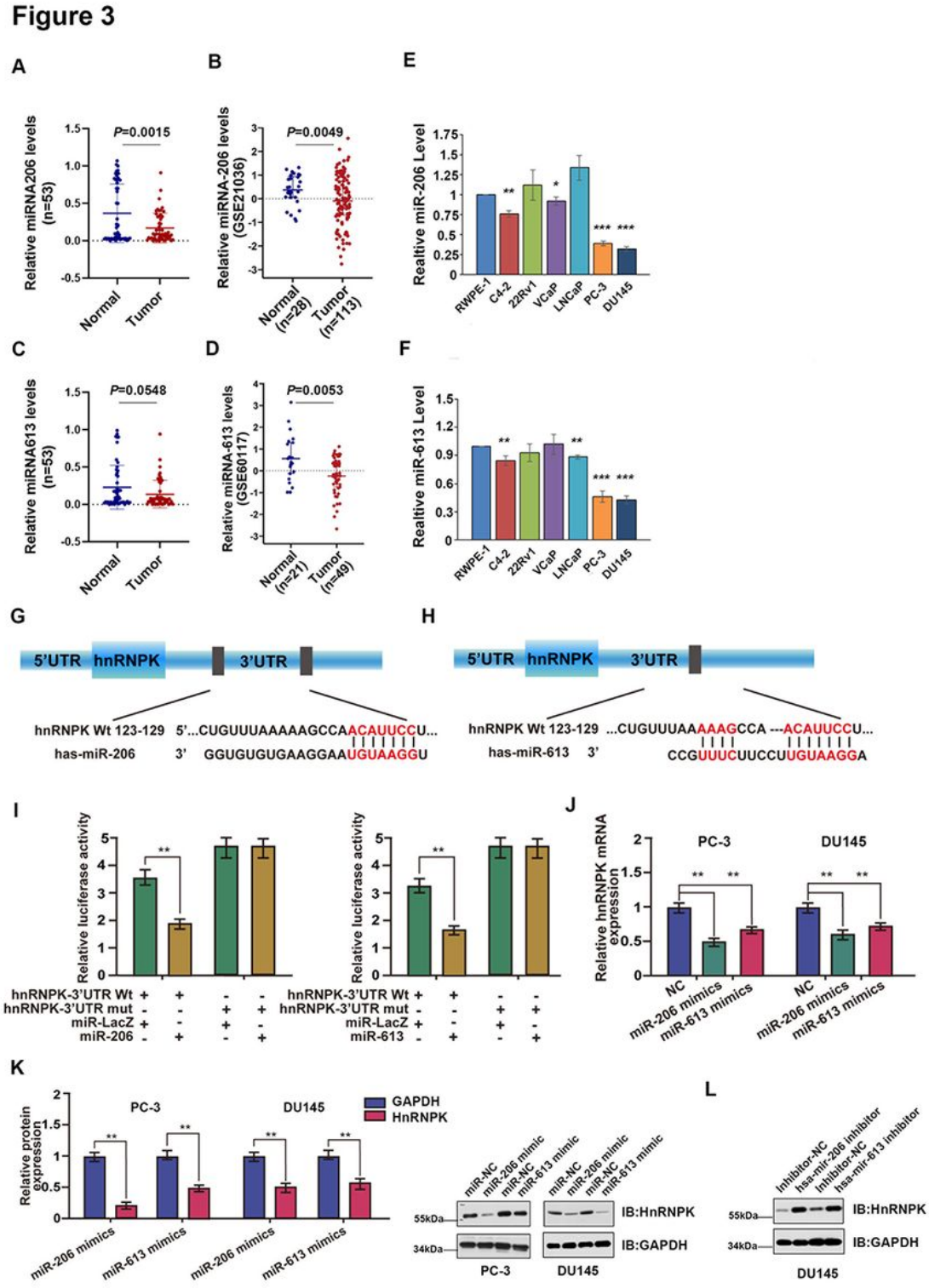

Figure 3

Mature miR-206 and miR-613 expression are decreased in PrCa, and directly targets the 3'-UTR of hnRNPK to decrease its expression. (A) Relative miR-206 and miR-613 (C) levels in 53 PrCa tissues and paired noncancerous Prostate tissues, U6 served as loading controls. (B) Scatter diagram showing

relative miR-206 and miR-613 (D) expression in PrCa tissues and adjacent normal prostate tissues from a public data set (GSE21036 and GSE60117). (E) RT-qPCR analysis of relative miR-206 and miR-613 (F) expression in human PrCa cell lines. (G and H) Schematic diagram of the predicted target binding sites of miR-206 and miR-613 in the 3′-UTR of hnRNPK. The seed recognition site is denoted. The nucleotides of the 3′-UTR region of hnRNPK that binds with miR-206 and miR-613 are highly conserved across species as predicated by TargetScan (http://www.targetscan.org/vert_71/). (I) The luciferase activity of the wild type hnRNPK 3'-UTR (Wt) and mutant hnRNPK 3'-UTR (Mut) co-transfected with miR-206/miR-613 mimics or a miRNA negative control (miR-LacZ) was measured in DU145 cells. Relative luciferase activity was plotted as the mean ± S.D of three independent experiments. (J and K) Expression of hnRNPK in PrCa cells line transfected with miR-206/miR-613 mimics or inhibitor (L) was detected by RT-qPCR and Immunoblot analysis respectively. Error bars represent the mean ± S.D of three independent experiments. *P<0.05, **P<0.01, ***P<0.001.

Figure 4

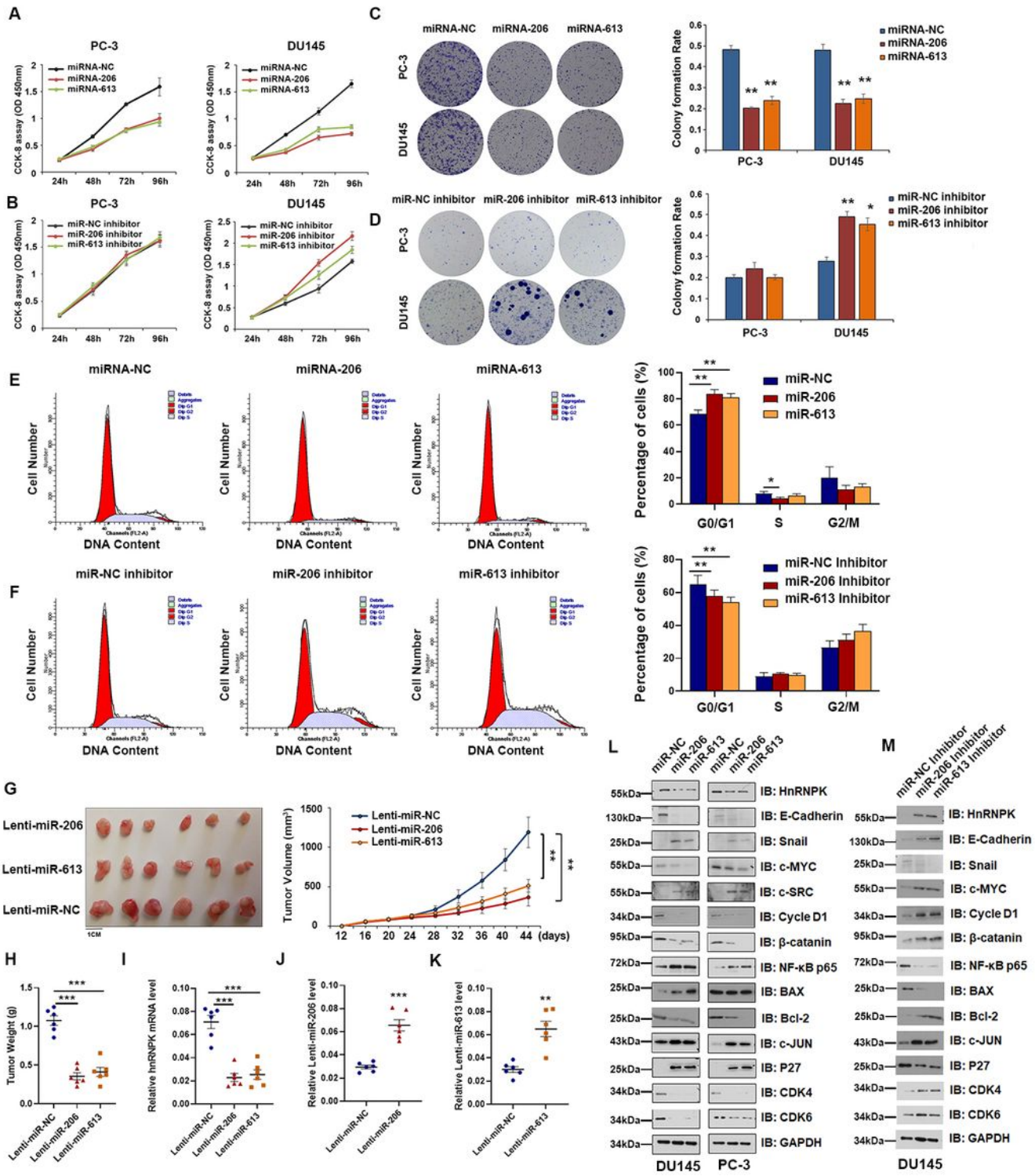

Figure 4

Overexpression of miR-206 and miR-613 inhibits cell growth and cell cycle in vitro and in vivo (A and B) CCK-8 assay of cell viability in PrCa cell lines transfected with miR-206, miR-613 mimics or miR-206, miR-613 inhibitor at 24, 48, 72 and 96 h. (C) Representative micrographs and (D) relative quantification of crystal violet-stained cell colonies analyzed by clongenic formation.(E and F) Flow cytometric analysis of DU145 cell lines. Cells were harvested at 72 h after transfection with the indicated miRNA and stained

with propidium iodide. The percentage of cells in each cell cycle phase is shown in the inset of each panel. (G) miR-206 and miR-613-overexpressed DU145 cell xenografts in nude mice (n=6) at the experimental endpoint, tumors were dissected and photographed as shown. Tumor growth curves in mice inoculated with the indicated cells at the indicated days. (H) Each tumor formed was weighed. (I-K) hnRNPK mRNA and miR-206, miR-613 expression in tumors was detected by qRT-PCR analysis. (L and M) The PC-3 and DU145 cells were treated with or without miR-206, miR-613 mimics or the miR-206, miR-613 inhibitor for 72 h, respectively. The expression levels of indicated protein were analyzed by Immunoblotting. Results were plotted as the mean ± S.D of three independent experiments. *P<0.05, **P<0.01, ***P<0.001.

Figure 5

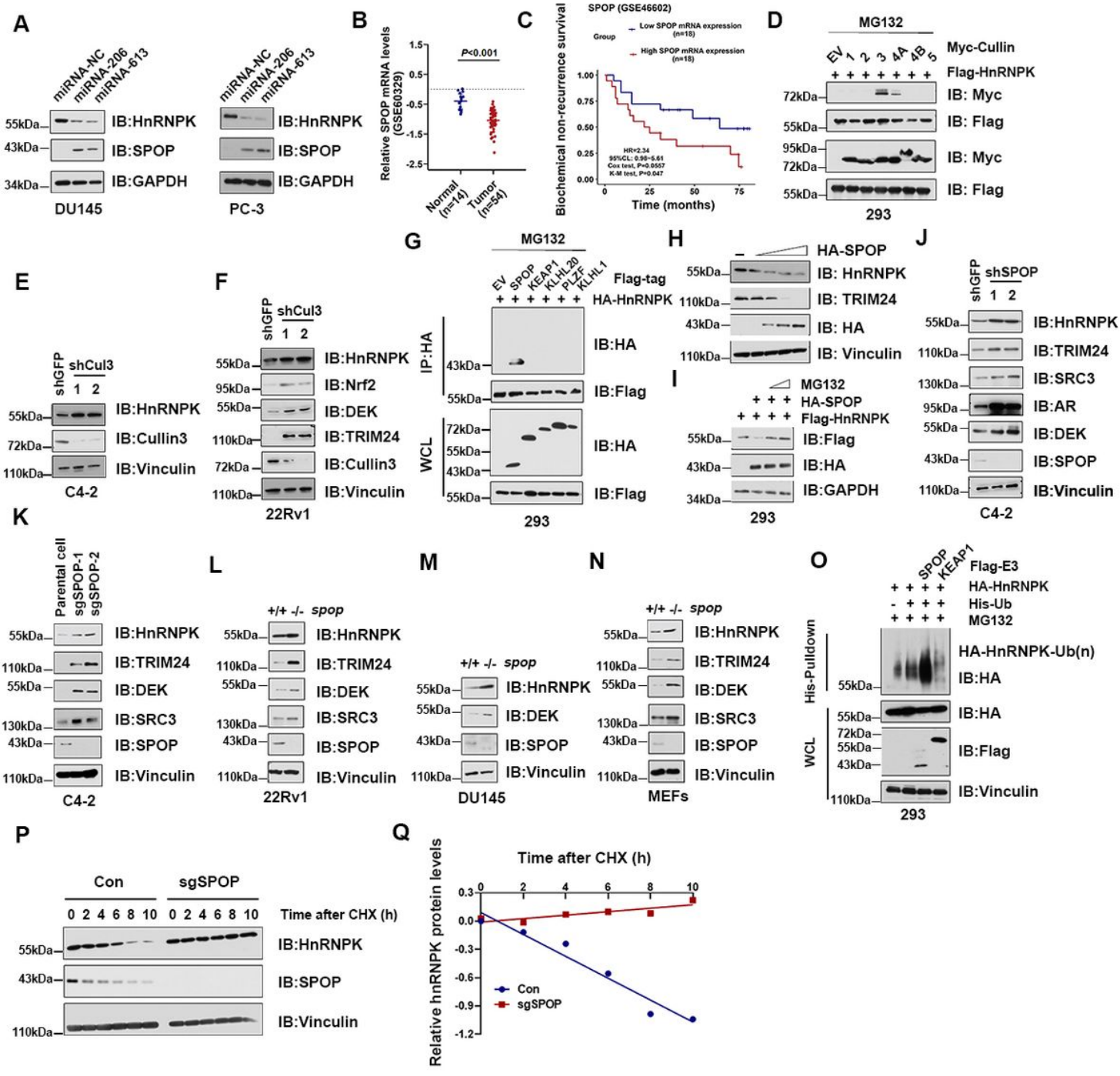

Figure 5

The Cullin 3 SPOP E3 ubiquitin ligase negatively regulates the stability of HnRNPK (A) Expression of HnRNPK and SPOP in PrCa cells transfected with miR-206 and miR-613 mimics was detected by Immunoblot analysis. (B) Relative SPOP mRNA expression levels in PrCa tissues and adjacent normal prostate tissues in a public data set (GSE60329).(C) Effect of the SPOP expression level on Biochemical recurrence in 36 prostate cancer patients who did not undergo androgen deprivation therapy, chemotherapy, radiotherapy or other anticancer treatment was analyzed, and Kaplan-Meier plots were generated using a Kaplan-Meier Plotter.(D) WB analysis of WCL and immunoprecipitates (IP) derived from 293 cells transfected with Flag-HnRNPK and various Myc-tagged Cullin constructs. 30 hours post-transfection, cells were treated with 10 μM MG132 for 10 hours before harvesting. (E) WB analysis of WCL derived from C4-2 and 22Rv1 (F) cells infected with the indicated lentiviral shRNAs. Infected cells were selected with 1 μg/ml puromycin for 72 hours to eliminate non-infected cells before harvesting. (G) WB analysis of WCL and IP derived from 293 cells transfected with HA-HnRNPK and Flag-tagged BTB domain-containing protein constructs. 30 hours post-transfection, cells were treated with 10 μM MG132 for 10 hours before harvesting. EV, empty vector. (H) WB analysis of WCL derived from C4-2 or 293 (I) cells transfected with increasing doses (0.5–3μg) of indicated plasmids. Where indicated, 10 μM MG132 was added for 10 hr before harvesting. (J) WB analysis of WCL derived from C4-2 cells infected with the indicated lentiviral shRNAs. Infected cells were selected with 1 μg/ml puromycin for 72 hours to eliminate non-infected cells before harvesting. (K-N) IB analysis of WCL derived from C4-2, 22Rv1,DU145 and mouse embryonic fibroblasts (MEFs) cells with SPOP knockout by the CRISPR technology.(O) WB analysis of WCLs and His pull-down products derived from 293 cells transfected with indicated constructs and treated with MG132 (10μM) 10 h. (P) SPOP knockout cells (sg SPOP) as well as parental C4-2 cells (Con) were treated with 100μg/ml cycloheximide (CHX), and cells were harvested at the indicated time points. Relative hnRNPK protein abundance was quantified by Image J and plotted in (Q). Data was shown as mean ± SD for three independent experiments. *P<0.05, **P<0.01, ***P<0.001.

Figure 6

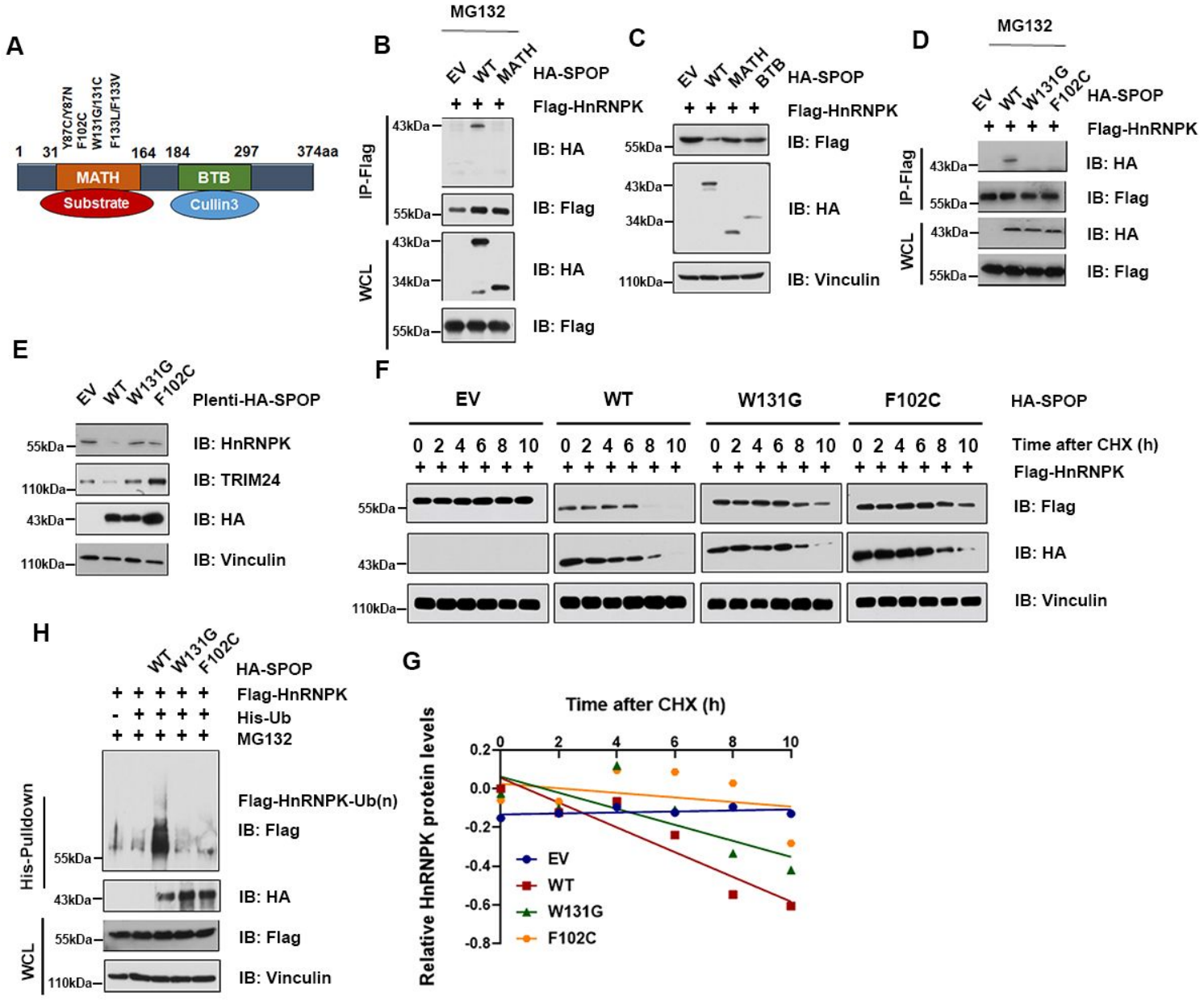

Figure 6

Prostate cancer-associated SPOP mutants impair to interact with and degrade HnRNPK (A) A schematic illustration of SPOP domains and prostate cancer-associated mutations. (B) WB analysis of WCL and immunoprecipitates derived from 293 cells transfected with Flag-HnRNPK and HA-SPOP-WT or deletion of MATH domain-SPOP constructs. 30 hours post-transfection, cells were treated with 10 μM MG132 for 10 hours before harvesting. EV, empty vector. (C) WB analysis of WCL derived from 293 cells transfected with indicated plasmids. (D) WB analysis of WCL and IP derived from 293 cells transfected with HA-SPOP-WT or prostate cancer -associated SPOP mutants. Cells were treated with 10 μM MG132 for 10 hours before harvesting. (E) WB analysis of WCL derived from C4-2 cells stably expressing HA-SPOP-WT or PrCa-associated SPOP mutants. (F) 293 cells transfected with Flag-HnRNPK together with the indicated HA-SPOP expressing plasmids. 30 hours post-transfection, cells were treated with 100 μg/ml

CHX for the indicated time period before harvesting. Relative Flag-hnRNPK protein abundance was quantified by Image J and plotted in (G). (H)WB analysis of WCLs and His pull-down products derived from 293 cells transfected with indicated constructs and treated with MG132 (10μM) 10 h.

Supplementary Files

This is a list of supplementary files associated with this preprint. Click to download.

- SupplementTable1.doc
- SupplementTable2.docx
- Supplementfigure1.tif
- Supplementfigure2.tif
- SupplementFigure.3.tif